Energy Conversion and Management: X 30 (2026) 101714

Contents lists available at ScienceDirect

Energy Conversion and Management: X

journal homepage: www.sciencedirect.com/journal/energy-conversion-and-management-x

Soot formation and ignition properties of diesel fuels with solketal in an injection chamber

Julian Türck [a,b,*], Sebastian Riess [c], Lukas Strauß [c], Fabian Schmitt [b], Ralf Türck [b,d], Wolfgang Ruck [a], Michael Wensing [c], Jürgen Krahl [d,e]

[a] Leuphana Universität Lüneburg, Universitätsallee 1, 21335 Lüneburg, Germany
[b] Tecosol GmbH, Jahnstraße 2, 97199 Ochsenfurt, Germany
[c] FAU Erlangen-Nürnberg, Cauerstraße 4, 91058 Erlangen, Germany
[d] Fuels Joint Research Group, www.fuels-jrg.de, Germany
[e] OWL University of Applied Sciences and Arts, Campusallee 12, 32657 Lemgo, Germany

ARTICLE INFO

Keywords:
Injection chamber
Solketal
Soot reduction
Influence of chemical structure
Diesel R33

ABSTRACT

The global energy transition drives an enhanced emphasis on innovative fuel design approaches. Novel renewable fuel components are being sought that are drop-in compatible and exhibit synergistic interactions within fuel components. Isopropylidene glycerin (solketal) is a promising candidate, offering favorable chemical and physical properties due to its high molecular oxygen content. This study investigates the soot formation tendency and ignition behavior of solketal in a high pressure and high temperature injection chamber. Its combustion characteristics under varying injection parameters and chemical influences were evaluated in comparison with 1,3-dioxolane and a reference fossil diesel fuel. Additionally, the influence of solketal in a binary biodiesel-solketal system and in Diesel R33 was examined. Solketal exhibited a soot-reducing effect alongside an increased ignition delay. Comparison with 1,3-dioxolane suggests that the enhanced oxidative reactivity is attributable to the hydroxyl functionality. This interpretation is supported by low-temperature combustion indicators and observations in the biodiesel-solketal system. The Diesel R33 results showed that a concentration of 3 wt% solketal provides the most favorable performance characteristics. This demonstrates how targeted blending strategies can unlock beneficial combustion effects. Such insights open promising pathways for developing advanced, future-ready fuel formulations.

1. Introduction

Optimizing diesel fuels for existing fleets has the potential to reduce greenhouse gas emissions in the short term. It is also possible to shift the energy industry towards a future without fossil fuels while reducing dependence on it. The property of a diesel fuel that allows it to be used in existing fleets is known as drop-in capability. Drop-in capability is determined by the physical and chemical properties of the fuel [1] and its compatibility with the engine (e.g. with elastomers [2], deposits on injection nozzles [3], etc.). An example of a defossilized drop-in fuel is Diesel R33 [4]. This fuel consists of 26 % hydrotreated vegetable oils (HVO), 7 % biodiesel and 67 % fossil diesel fuel. This fuel has been shown to increase the cetane number and thus reduce the ignition delay [5] and hydrocarbon emissions [4]. Furthermore, a reduction in soot formation was observed [5]. In order to further expand the potential in terms of soot formation and ignition behavior, polar drop-in components have come into focus. One example of this is polyoxymethylene ether (OME), which burns almost completely without forming soot [6]. Another promising group of compounds are alcohols, which, in the form of ethanol and methanol, have been shown to reduce soot-related emissions during combustion in gasoline engines [7,8]. Alcohols also show promising properties in diesel fuels. Investigations using 1-octanol as a fuel component have shown that diesel engine combustion can be achieved while lowering soot emissions [9].

The search for other sources of alcohol has brought glycerine into consideration. Glycerine is a by-product of biodiesel production and cannot be added to diesel fuels due to acrolein emissions[10], corrosion [11] and poor miscibility [12]. Chemical derivatization is required to make glycerine suitable for use as a diesel fuel. One possible route for the valorization of glycerine is its conversion to solketal [13] (see Fig. 1).

* Corresponding author at: Leuphana Universität Lüneburg, Universitätsallee 1, 21335 Lüneburg, Germany.
E-mail address: julian.tuerck@stud.leuphana.de (J. Türck).

https://doi.org/10.1016/j.ecmx.2026.101714
Received 5 November 2025; Received in revised form 14 February 2026; Accepted 24 February 2026
Available online 26 February 2026

Solketal is a bifunctional molecule that has both a hydroxy group and a dioxolane functionality. The constitutional isomer dioxane is also formed during production, typically in a 99:1 ratio relative to the dioxolane isomer [14]. Investigations on 1,3-dioxolanes associated with fuels are described in detail in the literature. These results indicate that 1,3-dioxolane exhibits gasoline-like ignition behavior, consistent with its reported low cetane number (~30) and corresponding resistance to compression ignition [15]. Because of the oxygen content of 1,3-dioxolane, oxygen enrichment occurs in both gasoline and diesel engines. During diesel combustion, both intake oxygen enrichment and fuel oxygenation effectively reduce particulate matter (PM) emissions, with oxygenated fuels providing substantial PM reductions. However, intake oxygen enrichment significantly increases NO_x emissions due to higher oxygen availability and/or higher combustion temperatures that promote thermal NO_x formation [15]. Based on 1,3-dioxolane, fuel studies have been conducted which show that solketal can be used both as gasoline [16] and diesel fuel [17]. It tends to increase the octane number [18], while at the same time lowering the cetane number [19]. It also increases storage stability by slowing down the oligomerization of biodiesel through reaction with epoxide precursors [20] and reduces gum formation in otto fuels [18]. Furthermore, solketal demonstrates synergistic effects that increase the effectiveness of antioxidants [21]. In terms of solketal's drop-in capability, injection and spray tests showed that solketal behaves like conventional fuels [22]. In general, a reduction in the cetane number leads to an increase in the ignition delay [23].

Prolonged ignition delay can increase unburned hydrocarbon emissions, indicating a higher tendency toward incomplete combustion [24]. The fuel mixture can become overly lean and widely distributed before ignition, limiting oxidation of fuel to completion [25]. Furthermore, a long ignition delay can promote incomplete combustion by increasing fuel-wall interaction prior to ignition, which enhances quenching and leaves part of the fuel insufficiently oxidized [26]. Conversely, longer ignition delay can also allow more time for fuel and air to mix before auto-ignition [27]. This larger premixed burn is typically associated with higher local peak temperatures early in combustion, which can enhance thermal NO_x formation [28]. Initial evidence for evaluating ignition and combustion characteristics is obtained from tests in injection chambers. These tests can detect soot incandescence and OH* radical chemiluminescence, which in turn helps to determine ignition delays. Depending on these parameters, lift-off lengths (LOL) and timing can also be examined. These parameters can be used as an indicator to investigate how the fuel is mixed with oxygen [29]. A higher LOL, which correlates with a greater distance from the injection nozzle, results in better fuel–air mixing. However, no statements can be made about the global equivalence ratio or the jet momentum. Since matter emits temperature-dependent electromagnetic radiation, it is feasible to measure the radiation from soot [30]. This is achievable due to the temperature during diesel combustion at temperatures of up to 2600 K [31]. Another parameter for determining the tendency to form soot is the chemiluminescence of OH* radicals [32]. In principle, a higher concentration of OH* radicals can be the result of a larger amount of oxygen [33]. However, studies have shown that OH* radicals produce precursors for soot formation mainly for polyaromatic hydrocarbons [34]. In addition, Hardalupas et al. demonstrated that the intensity of OH* chemiluminescence depends on fuel mass flow rate, equivalence ratio, and turbulence in the same manner as the heat release rate, supporting the use of OH* as a representative indicator of heat release [35].

This work deals with the influence of solketal on diesel fuels in a high-temperature and high-pressure injection chamber, which represents the behavior of the fuel at the moment of ignition. These experiments are intended to investigate the potential of solketal as a diesel fuel in terms of its tendency to form soot. For this purpose, the soot incandescense, OH* radical chemiluminescence, ignition delay and LOL were detected. First, a distinction is made between 1,3-dioxolan and solketal and their influence on reference fossil diesel fuel is investigated. Subsequently, investigations are carried out in a binary system with biodiesel and Diesel R33.

2. Experimental section

2.1. Fuels and chemicals

Analytical data for the fuel properties are provided in the Supporting Information. Solketal (98 % purity) was obtained from Merck KGaA, Germany. 1,3-Dioxolane (99.5 % purity) was supplied by Thermo Fisher Scientific Inc., USA. Biodiesel was sourced from Louis Dreyfus Company B.V., Netherlands, and HVO was procured from Shell plc, United Kingdom. The reference fossil diesel fuel was purchased from Haltermann Carless GmbH, Germany. The investigated fuel blends included binary mixtures of the reference diesel with either 3 wt% solketal or 3 wt % 1,3-dioxolane. In addition, solketal was blended with biodiesel in 5 wt % increments up to 25 wt%. Diesel R33 was also examined as a base fuel, blended with solketal at concentrations of 2, 3, 4, 6, and 9 wt%.

2.2. Test bench

The optical investigations are performed in a high-temperature, high-pressure injection chamber (see Fig. 2). During the experiment, the cubic chamber is continuously purged with pure air. Electric heaters located at the four upper corners of the chamber raise the gas temperature in three steps, enabling temperatures of up to 1,000 K in the injection-relevant region. The combination of controlled purge gas flow and an exhaust needle valve enables to set ambient pressures as high as 10 MPa. A research-grade fuel injection system, consisting of two

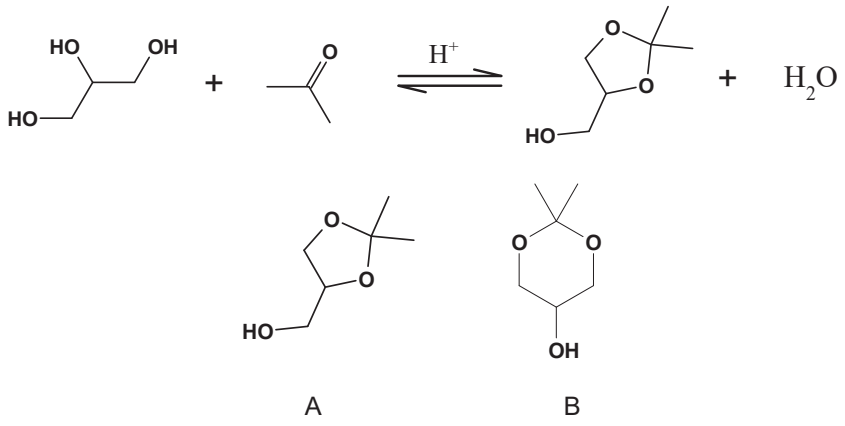

Fig. 1. Proton-catalyzed condensation reaction for the synthesis of solketal. The 5-membered ring represents dioxolane (A) and the 6-membered ring is the dioxane (B) isomer.

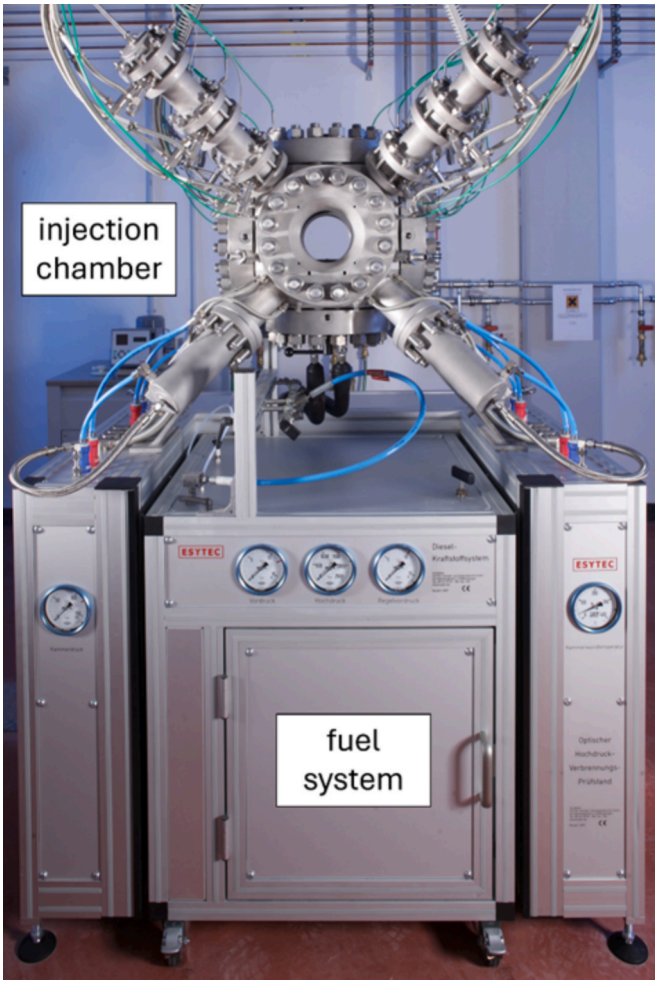

Fig. 2. High-temperature and high-pressure injection chamber with fuel supply system.

Maximator pressure amplifiers, supplies injection pressures up to 400 MPa with minimal fluctuation. Five sides of the vessel are fitted with optical access ports, each equipped with 125 mm diameter windows. The bottom flange incorporates an injector mounting system that also enables fuel and injector temperature control between 253 K and 373 K using a thermostat.

Due to the continuous pure air purge, the ambient pressure remains constant throughout the injection event. The resulting gas flow can be regarded as steady relative to the high injection velocities typical of diesel engine conditions. This constant purge also ensures the rapid removal of residual fuel, allowing tests to be conducted at a repetition rate of 1 Hz. Additional information is provided in [36].

All experiments utilize a modified, piezo-actuated common-rail injector with a servo-hydraulic control system. The injector is fitted with a customized research nozzle featuring three symmetrically arranged holes at a 45° elevation angle, enabling isolated observation of a single spray. Each nozzle orifice has a diameter of 115 µm, a length-to-diameter ratio of 6.5, and a conicity factor of 2. The energizing duration for the presented measurements is 1.5 ms.

2.3. Optical setup

A Photron Fastcam SA-Z operating at 50,000 fps is used to record the natural luminosity of the spray flames in the visible spectrum. This emission is primarily caused by thermal radiation from soot and serves as an indicator of the sooting propensity of the tested fuel mixtures. In parallel, a second Fastcam SA-Z equipped with a LaVision IRO X high-speed intensifier captures ultraviolet emissions at the same frame rate, with a spectral sensitivity of ± 25 nm around a center wavelength of 307 nm. During ignition and premixed combustion, this UV signal is dominated by chemiluminescence of OH* radicals, which mark the high-temperature combustion regime. In the subsequent non-premixed phase, UV emission becomes significantly affected by soot radiation.

For each operating condition, 32 individual injections and combustion events are recorded to facilitate statistically robust analysis. The onset of OH*-related UV emission is statistically evaluated to determine the ignition delay time (t_{ID}), while an equivalent analysis of visible light emission is used to determine the soot signal delay (t_{SD}) [36]. Additionally, LOL and penetration depth are extracted for both signals. Penetration depth is defined as the farthest detected signal location relative to the nozzle exit, and LOL as the closest detected combustion signal location. Further details on the image processing are given in [36]. The error was determined for the LOLs and the signal and ignition delay. For these parameters, example plots of the error used in the discussion are shown in the Supporting Information. However, the soot incandescense and OH* radicals could not be statistically evaluated, as this is an evaluation in which the parameters are determined by addition.

For each recorded time step, a mean intensity image is calculated from the 32 events, and the pixel intensities are integrated to form temporal intensity traces, as illustrated in Fig. 2. For the UV signal (Fig. 3, left), the maximum intensity during the premixed phase (up to roughly 950 µs in the given example) is used as an indicator of fuel reactivity under the respective boundary conditions. Experimental and numerical studies have shown that the spatial and temporal evolution of OH* emission closely follows the onset and development of high-temperature combustion chemistry, making it a reliable indicator of ignition and reaction-zone progression in both premixed and non-premixed combustion systems [37,38]. Later peaks dominated by soot radiation (beyond approximately 950 µs) are excluded. For the visible signal (Fig. 3, right), the maximum intensity is evaluated as a measure of soot formation intensity.

2.4. Test conditions

The operating conditions are derived from the Spray A reference case of the Engine Combustion Network (ECN) and include variations of injection pressure, ambient pressure and temperature, as well as fuel temperature, as summarized in Table 1. For all experiments presented, the chamber is filled with pure air (21 % oxygen).

3. Results and discussion

In general, the diagrams for the various conditions for both soot and OH* radicals, which are not shown in this section, are displayed in Supporting Information. The same applies to the LOL as well as to the signal and ignition delays.

3.1. Influence of injection parameters on ignition properties by means of 1,3-dioxolane and solketal

Neither solketal nor 1,3-dioxolane could be ignited in this experimental setup, which is due to a high octane number and the resulting lower cetane number [39]. In order to evaluate the solketal effect, the two polar molecules had to be blended with diesel fuels. These served as cetane number enhancers. Therefore, both molecules were blended into a reference fossil diesel fuel at a concentration of 3 wt% and compared with the pure fuel. The soot incandescense was initially compared while the ambient conditions, injection pressure and fuel temperature were varied. Figs. 4 and 5 show examples of the graphs at ambient conditions of 62 °C and 627 bar, with an injection pressure of 1500 bar and a fuel temperature of 90 °C.

The tables containing the values evaluated for the physical

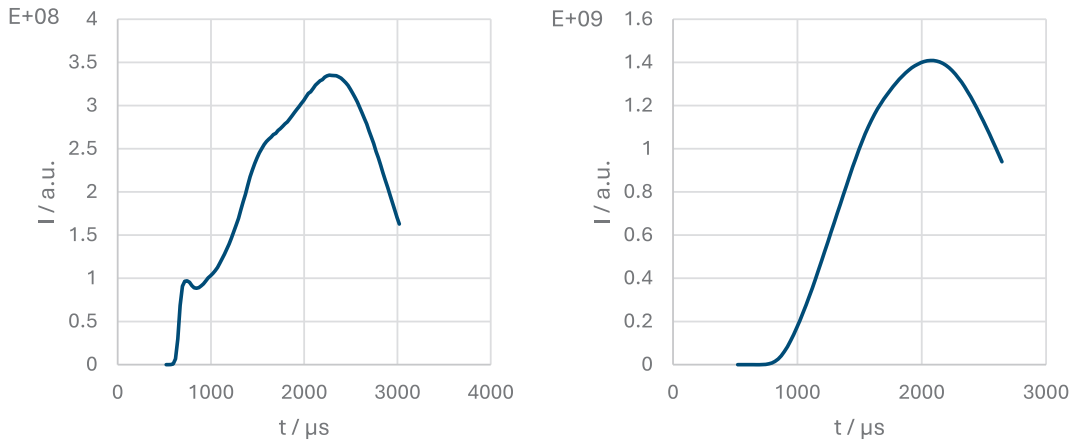

Fig. 3. Exemplary intensity traces of the UV signal (left) and the visible signal (right) for pure fossil diesel fuel at 62 bar ambient pressure, 627 °C ambient temperature, 1,500 bar injection pressure and 90 °C fuel temperature.

Table 1
Operating conditions for the optical investigations.

Ambient pressure [bar]	Ambient temperature [°C]	Ambient density [kg/m^3]	Injection pressure [bar]	Fuel temperature [°C]
59	577	22.8	1,500	90
62	627	22.8	500	90
62	627	22.8	1,000	90
62	627	22.8	1,500	90
62	627	22.8	1,500	−20
62	627	22.8	1,500	25
62	627	22.8	1,500	90
66	677	22.8	1,500	90

conditions are included in the Supporting Information. Based on these values, the Tables 2 and 3 show the factors for the increase or decrease in both soot incandescense and OH* radical chemiluminescence. Two peaks appear during the progression of OH* radicals. The small peak at the front is the peak of premixed combustion, while the larger peak that follows is the peak of diffusive combustion [40]. The peak of diffusive combustion is neglected in the following. This is because soot radiation has a broadband signal that extends into the UV range. This has an influence on the OH* radical signal. The peak of premixed combustion is therefore taken into account.

As ambient conditions increase, soot incandescense increases while the chemiluminescence of OH* radicals decreases. The strongest increase in soot incandescense is observed for fuels between 59 bar, 577 °C and 62 bar, 627 °C, with solketal showing the strongest increase (10.25), followed by reference diesel (6.44) and 1,3-dioxolane (3.48). This steep increase is also due to the fact that the value of solketal at 59 bar and 577 °C is significantly lower than that of reference fossil diesel fuel and 1,3-dioxolane. The increase to 66 bar and 677 °C then shows a smaller increase and settles in the range of 2.7 to 3.5 for the three fuel blends. The OH* radicals show decreases in the range of 0.7 to 0.9 for all three fuel mixtures. Solketal exhibits the lowest soot incandescense and OH* radical chemiluminescence in the low-energy range. A proportionality was observed in the ignition and signal delay, with a reduction of 0.7 for all fuels under varying ambient conditions. The increased thermodynamic conditions also play a role, leading to faster ignition due to the higher energy conditions. Furthermore, no fuel-related influence can be determined here [41]. This faster ignition results in less mixing of fuel and air, which ultimately leads to an increase in the soot signal. Furthermore, premixed combustion provides less time for OH* radicals to form.

When the injection pressure varies, an influence on soot incandescense, OH* radical chemiluminescence and the delays can be observed. An increase can be observed from 500 to 1,000 bar, with OH* radicals increasing by 1.43 for the reference fossil diesel fuel. For solketal and

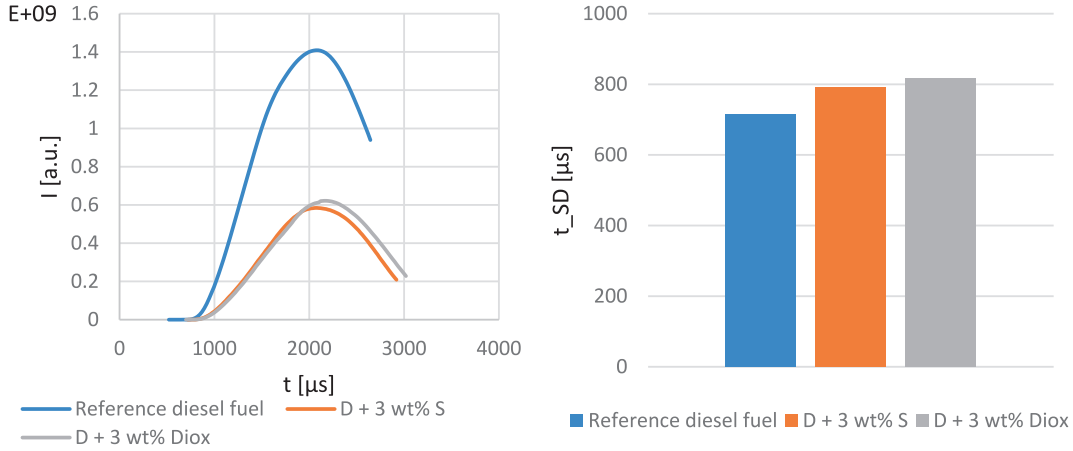

Fig. 4. Progression of soot incandescense (left) and the signal delay of soot incandescense for reference fossil diesel fuel (blue), reference fossil diesel fuel (D) + 3 wt % solketal (S, orange) and D + 3 wt% dioxolane (Diox, grey). The injection parameters ambient conditions of 62 bar and 627 °C, with an injection pressure of 1500 bar and a fuel temperature of 90 °C. The energizing time conducted 1500 µs. (For interpretation of the references to colour in this figure legend, the reader is referred to the web version of this article.)

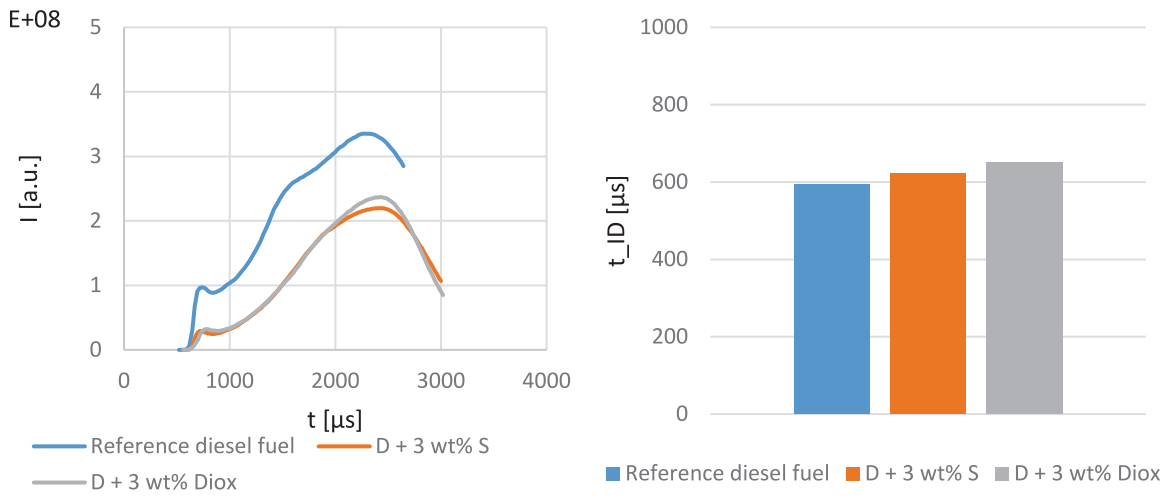

Fig. 5. Progression of OH* radicals (left) and the ignition delay for reference fossil diesel fuel (blue), reference fossil diesel fuel (D) + 3 wt% solketal (S, orange) and D + 3 wt% dioxolane (Diox, grey). The injection parameters ambient conditions of 62 bar and 627 °C, with an injection pressure of 1500 bar and a fuel temperature of 90 °C. The energizing time conducted 1500 µs. (For interpretation of the references to colour in this figure legend, the reader is referred to the web version of this article.)

Table 2
Illustration of the influence of changes in injection parameters, ambient conditions, injection pressure and fuel temperature. The factors are displayed for soot incandescense and OH* radicals in the blends reference fossil diesel fuel D + 3 wt% S and D + 3 wt% diox. The factor refers to the solketal blend, which means that <1 represents a decrease and >1 represents an increase.

Factors	Reference diesel fuel		D + 3 wt% S		D + 3 wt-% Diox.	
Ambient conditions	Soot Incandescense	OH* radical	Soot Incandescense	OH* radical	Soot Incandescense	OH* radical
59 bar, 577 °C –> 62 bar, 627 °C	6.44	0.89	10.25	0.74	3.48	0.74
62 bar, 627 °C –> 66 bar, 677 °C	2.71	0.80	3.45	0.82	2.98	0.83
Injection pressure	Soot Incandescense	OH* radical	Soot Incandescense	OH* radical	Soot Incandescense	OH* radical
500 –>1,000 bar	0.52	1.43	0.52	1.51	0.55	1.51
1,000 –> 1,500 bar	0.88	1.40	0.43	1.45	0.43	1.36
Fuel temperature	Soot Incandescense	OH* radical	Soot Incandescense	OH* radical	Soot Incandescense	OH* radical
20 –> 25 °C	1.36	1.22	0.96	1.91	0.95	1.82
25 –> 90 °C	2.97	1.05	2.10	0.97	2.06	0.95

Table 3
Illustration of the influence of changes in injection parameters, ambient conditions, injection pressure and fuel temperature. The factors are displayed for the ignition and signal delay for soot incandescense and OH* radicals in the blends reference fossil diesel fuel D + 3 wt% S and D + 3 wt% diox.

Factors ignition/signal delay	Reference diesel fuel		D + 3 wt% S		D + 3 wt-% diox.	
Ambient conditions	Soot Incandescense	OH* radical	Soot Incandescense	OH* radical	Soot Incandescense	OH* radical
59 bar, 577 °C –> 62 bar, 627 °C	0.69	0.69	0.72	0.74	0.70	0.71
62 bar, 627 °C –> 66 bar, 677 °C	0.70	0.70	0.72	0.72	0.72	0.71
Injection pressure	Soot Incandescense	OH* radical	Soot Incandescense	OH* radical	Soot Incandescense	OH* radical
500 –> 1,000 bar	0.88	0.87	0.95	0.97	0.96	0.95
1,000 –> 1,500 bar	0.96	0.95	0.99	0.97	0.98	0.96
Fuel temperature	Soot Incandescense	OH* radical	Soot Incandescense	OH* radical	Soot Incandescense	OH* radical
−20 –> 25 °C	0.89	0.85	0.95	0.96	0.94	0.94
25 –> 90 °C	0.86	0.86	0.99	0.97	0.93	0.93

1,3-dioxolan the increase conducts 1.51. In all three blends, the soot incandescense decreases by a factor of between 0.4 and 0.9. An increase in injection pressure leads to a higher mass flow rate [42] and a higher fuel velocity [43]. This increase should lead to more fuel–air mixing and thus influences soot incandescense and OH* radical chemiluminescence.). Since the local fuel–air ratio is constant and the higher mass flow rates result in more fuel entering the combustion chamber, while the ignition delays change comparatively less, combustion at higher injection pressures is leaner. This leads to more premixed combustion, which is noticeable through an increase in OH* radicals. As a result, soot formation decreases (0.88 to 0.97). The increased fuel velocity leads to faster formation of a fuel–air mixture that has a sufficient

ignition temperature.

When the fuel temperature varies from −20 °C to 25 °C, increases can be observed in the reference diesel (soot incandescense: 1.36 OH* radical: 1.22 %). With solketal and 1,3-dioxolane, on the other hand, slight decreases in soot incandescense (0.96 and 0.95 %) and significant increases in OH* radical chemiluminescence (1.91 and 1.82) are observed. The fact that solketal and 1,3-dioxolane cause a slight reduction in soot incandescense but increase OH* chemiluminescence indicates an increase in reactivity due to blending. When the temperature increases to 90 °C, soot incandescense increase in all three blends in the range from 2 to 3. The OH* radical chemiluminescence decreased from 0.8 to 0.95. The reference fossil diesel shows the strongest increase, which could be a further indication of a reduction in soot due to 1,3-dioxolane and solketal. A comparison between 1,3-dioxolane and solketal shows that both exhibit a similar increase in soot incandescense. With regard to the delays, reductions are observed with increasing temperature, as the fuel is more reactive [44] and mixes better with air [45].

Another factor, which is influenced by the ignition properties, is the LOL. It is determined for both soot incandescense and OH* radicals. Fig. 6 shows two LOL diagrams for soot incandescense and OH* radicals as examples. The values are listed for all physical parameters in the Supporting Information. The factors caused by the changes are listed in Table 4. In general, the individual values of the LOL for the OH* radicals are shorter in all sections compared to the LOL of the soot incandescense. This is due to the evaluation of the OH* radicals, which also locally represents the pre-mixed combustion before transitioning to a diffusion-controlled combustion.

With regard to the ambient conditions, it is immediately apparent that the LOL for both, OH* radicals and soot incandescense decrease between 0.75 and 0.85. This is related to ignition delays, as faster ignitions give the fuel less time to move away from the injection nozzle. When the injection pressure changes, the LOL behaves differently. As the injection pressure increases, the LOL increases due to the greater mass flow (1.16 to 1.51). This is another observation that better mixing is taking place, which correlates with the observation of soot incandescense and OH* radical chemiluminescence. When the fuel temperature varies, it becomes apparent that this has no significant influence on the LOL. Due to the decrease in ignition delay, it can be seen that ignition occurs faster with similar lengths. This also highlights the fact that the blends ignite more quickly due to the change in thermodynamics rather than due to the injection.

3.2. Comparison of fuel dependent ignition behavior between 1,3-dioxolane and solketal

After evaluating the variation in the injection parameters, the influence of the fuel is discussed in the following. For this purpose, the factors relating to the ratios between solketal and the reference diesel or solketal and 1,3-dioxolane are presented in Tables 5 and 6. Since the ignition delay and the signal delay are correlated, only the ignition delay was taken into account in the following. Since the ignition delay is determined based on OH* radical chemiluminescence, only the OH* radical parameter is referenced for the LOL. The comparison with regard to premix combustion was carried out in Section 3.1.

The comparison between the reference fossil diesel fuel and solketal shows a fundamental trend. In general, soot incandescense decreases significantly under all physical injection conditions. An even stronger decrease can be observed for OH* radicals. As both parameters decrease significantly, it can be assumed that Solketal has a soot-reducing effect. The observation that soot-related parameters decrease is consistent with the assumption that the higher molecular oxygen density reduces the tendency to form soot. Furthermore, the addition of solketal reduces the concentration of soot forming particles in the reference fossil diesel fuel, such as polyaromatic hydrocarbons46. It is striking that significant reductions are already measured with 3 wt% solketal. Emission tests already carried out in the literature also confirm that solketal reduces soot [47]. This could be due to a low number of C-C bonds and the absence of double bonds [48]. However, in terms of ignition delay, the reference diesel ignites faster, apart from the following injection parameters: These are the ambient conditions at 59 bar and 577 °C, low fuel temperatures of −20 and 25 °C and the injection pressure of 500 bar. These parameters represent less energy-intensive injections. As the values of these parameters increase, the ignition delay also increases when comparing solketal with the reference fossil diesel fuel. This observation correlates with the fact that solketal reduces the cetane number.

Considering the tendency for soot incandescence to decrease more strongly with increasing fuel temperature and injection pressure, it is conceivable that the influence of solketal increases, leading to a reduction in soot and a greater ignition delay. This is an initial indication that solketal is more reactive under conditions with lower thermodynamic condition or that reactivity increases with increasing value. This is particularly evident under ambient conditions of 59 bar and 577 °C, where a reduction of 74 % is achieved. The analysis of LOL provides an

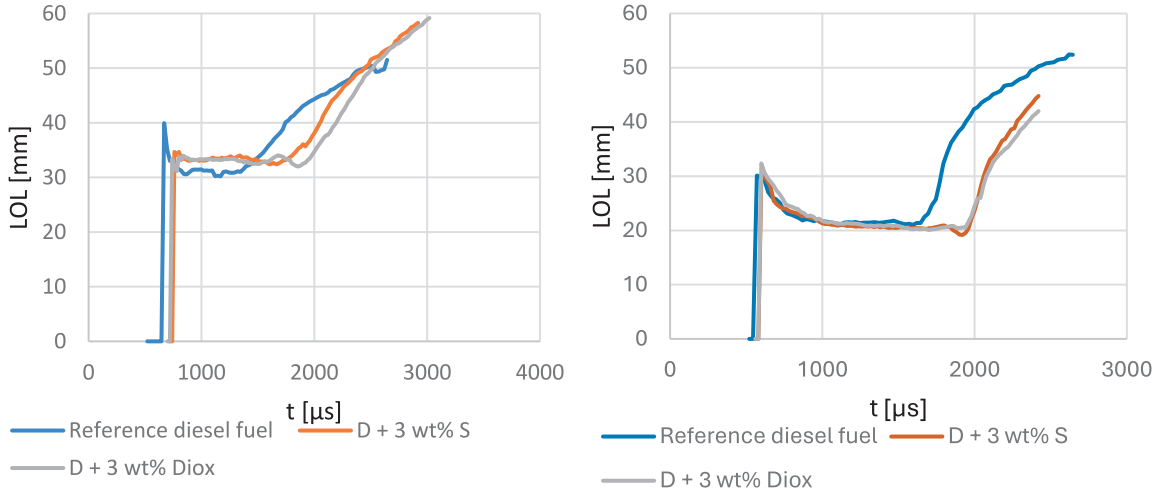

Fig. 6. The plots show the evolution of LOL for soot incandescence (left) and OH* radical chemiluminescence (right). The fuels tested were reference fossil diesel fuel (blue), D + 3 wt% S (orange) and D + 3 wt% diox (grey). The injection parameters ambient conditions of 62 °C and 627 bar, with an injection pressure of 1500 bar and a fuel temperature of 90 °C. The energizing time conducted 1500 µs. (For interpretation of the references to colour in this figure legend, the reader is referred to the web version of this article.)

Table 4
Factors which display the changes by varying injector parameters. The factors are displayed for LOL and time for soot incandescence in the blends reference fossil diesel fuel D + 3 wt% S and D + 3 wt% diox. The factor refers to the solketal blend, which means that <1 represents a decrease and >1 represents an increase.

Increase Liftoff	Reference diesel fuel		D + 3 wt% S		D + 3 wt% Diox.	
	Soot Incandescense	OH* radical	Soot Incandescense	OH* radical	Soot Incandescense	OH* radical
Ambient conditions	LOL [mm]	LOL [mm]	LOL [mm]	LOL [mm]	LOL [mm]	LOL [mm]
59 bar, 577 °C –> 62 bar, 627 °C	0.76	0.75	0.82	0.77	0.77	0.75
62 bar, 627 °C –> 66 bar, 677 °C	0.76	0.76	0.80	0.85	0.80	0.83
Injection pressure	LOL [mm]	LOL [mm]	LOL [mm]	LOL [mm]	LOL [mm]	LOL [mm]
500 –> 1,000 bar	1.51	1.30	1.43	1.20	1.44	1.25
1,000 –> 1,500 bar	1.16	1.20	1.23	1.21	1.21	1.17
Fuel temperature	LOL [mm]	LOL [mm]	LOL [mm]	LOL [mm]	LOL [mm]	LOL [mm]
20 –> 25 °C	1.00	1.00	1.02	0.96	1.07	1.02
25 –> 90 °C	1.00	1.00	1.05	0.95	1.04	0.95

Table 5
Ratio of soot incandescense, OH* radical chemiluminescence, signal delay and lift-off parameters between Solketal and the reference fossil diesel fuel. The factor refers to the solketal blend, which means that <1 represents a decrease and >1 represents an increase.

Ambient conditions	Soot incandescense	OH* radical	Ignition delay	LOL
59 bar, 577 °C	0.26	0.36	0.99	0.92
62 bar, 627 °C	0.41	0.30	1.05	0.95
66 bar, 677 °C	0.53	0.31	1.08	1.05
Injection pressure [bar]				
500	0.86	0.28	0.92	1.03
1000	0.85	0.29	1.03	0.95
1500	0.41	0.30	1.05	0.95
Fuel temperature				
20	0.84	0.21	0.83	1.05
25	0.59	0.33	0.94	1.00
90	0.41	0.31	1.05	0.95

Table 6
Ratio of soot incandescense, OH* radical chemiluminescence, ignition delay and lift-off length parameters between solketal and 1,3-dioxolane. The factor refers to the solketal blend, which means that <1 represents a decrease and >1 represents an increase.

Ambient conditions	Soot incandescense	OH* radical	Ignition delay	LOL
59 bar, 577 °C	0.32	0.90	0.92	0.97
62 bar, 627 °C	0.94	0.91	0.96	1.00
66 bar, 677 °C	1.09	0.90	0.97	1.02
Injection pressure [bar]				
500	1.00	0.85	0.92	1.01
1000	0.94	0.85	0.94	0.97
1500	0.94	0.91	0.96	1.00
Fuel temperature				
20	0.92	0.85	0.90	1.06
25	0.93	0.89	0.92	1.00
90	0.94	0.75	0.96	1.00

in-depth understanding of the influence of solketal on the reference fossil diesel fuel. The ratio of LOL increases, while the LOL decreases with higher ambient conditions. The situation is different for the injection pressure and the fuel temperature. The ratio of LOL decrease with increasing injection parameters. However, if the individual values are considered (see Supporting Information), it can be seen that the LOL rises for the injection pressure and stays unaffected by the fuel temperature. The fact that the LOL values here are opposite to the ignition delay indicates that Solketal has an influence. Later ignition should normally also lead to higher LOL values. In addition, the mixing should be less thorough. The fact that less soot was measured nevertheless indicates the oxidative behavior of solketal. This raises the question of whether solketal has a chemical or physical impact.

To gain an understanding of the impact, 1,3-dioxolane is compared with solketal in a similar manner. In general, the differences between solketal and 1,3-dioxolane are minor. It is evident that, as in the comparison with the reference fossil diesel fuel, a significant reduction in soot incandescense can be observed at an ambient pressure of 59 bar and an ambient temperature of 577 °C. This indicates a higher reactivity of solketal. As ambient conditions increase, the values of the two blends converge, as can be seen from the ratio, which is close to 1. Similar to the ambient conditions, the ratio approaches the value 1 when the injection pressure increases. When the fuel temperature varies, less signals tend to be formed with solketal. It can be seen that solketal generally forms less OH* radicals. This correlates with the ignition delay ratio, which indicates that solketal ignites more quickly under all conditions. The ignition delay is consistent for all parameters and is mostly within the range of 3–10 % below the value for 1.3-dioxolane. An exception is the fuel temperature of 90 °C, at which solketal exhibits significantly fewer OH* radicals (0.75) with a relatively similar ignition delay (0.96) and fewer soot incandescense (0.94). This is further evidence of the difference, which suggests that solketal is more reactive. In general, the LOL for all injection conditions show the same length. This means that the fuel–air mixture should be approximately the same. Since the ignition delays are shorter for solketal blends, this is another indication of increased reactivity. Therefore, the question arises as to which factor is decisive.

In order to assess whether the effect is chemical or physical, important physical parameters are first compared. The significant reduction in the low-energy area suggests that there should be an additional chemical influence. A shorter ignition delay can mean less effective premixing with oxygen [49]. Surface tension is in the same range, as it is 34.4 mN/m [50] for 1.3-dioxolane and 32.1 mN/m [51] for solketal (at 25 °C). The same applies to density, which is 1.06 kg/cm^3 (20 °C) for both. The dynamic viscosity is lower for 1,3-dioxolane at 0.55 mPas [50], while it is 11 mPas for solketal [52]. Due to the quantity of 3 wt%, the dynamic viscosity of solketal should not have a significant impact on injection. Berteau et al. demonstrate that 3 mL solution of 15–20 mPas of a component can be tolerated [53]. Furthermore, dynamic viscosity would have an influence on atomization, and in this case, reducing the viscosity with 1,3-dioxolane should lead to improved

soot formation tendency [54]. In general, the blending quantity of 3 wt % is within a range that makes physical influences unlikely. Therefore, the difference in chemical structure and thus the hydroxyl group becomes the centre of attention. In general, it is interesting that solketal forms less OH* radicals than 1,3-dioxolane. This means that the additional hydroxyl group in solketal does not automatically form more OH* radicals. Furthermore, it has been shown that higher molecular oxygen density does not automatically lead to more OH* radicals. However, various studies show that OH groups have a positive influence on the oxidation of hydrocarbons, e.g. by reducing soot activation energies [55] or by suppressing the growth of primary particles through oxidation [56]. In general, glycerol ketals and acetals show a reduction in particle emissions [57]. Nevertheless, a comparison between 1,3-dioxolan and solketal shows that the additional hydroxyl group has the potential to further minimize soot reduction. The fact that solketal appears to be more reactive in low-energy measurements, which correlates with the comparison with reference fossil diesel fuel, also indicates higher reactivity and thus an effect influenced by the hydroxyl group.

3.3. Influence of solketal on the ignition behavior of binary solketal biodiesel blends

After comparing 1,3-dioxolane and solketal, the influence of solketal on diesel fuels is now evaluated. First, binary biodiesel-solketal blends were analyzed. Since there is no immiscibility gap between biodiesel and solketal, larger quantities and generally higher concentrations can be mixed. However, there is an upper blending limit, as solketal does not ignite as a pure substance under diesel engine conditions. Pure biodiesel with 10 wt%, 15 wt%, 20 wt% and 25 wt% solketal was then investigated. The injection conditions were an ambient pressure of 62 bar, an ambient temperature of 627 °C, an injection pressure of 1,500 bar and a fuel temperature of 90 °C. Fig. 7 displays the progression of the soot incandescense and OH* radical chemiluminescence.

In general, the blends show that they ignite under diesel engine conditions despite the addition of 25 wt% of solketal. The trends for soot incandescense and OH* radicals both show a reduction compared to pure biodiesel. For the soot incandescense a slight decrease from 0 to 10 wt% solketal (1.12) and a significant decrease was observed in the jump from 10 to 15 wt% (4.34). At 20 and 25 wt%, the curve flattens slightly but still shows two orders of magnitude less soot intensity than pure biodiesel. The OH* radicals decrease constantly up to 15 wt% solketal (1.79) and then increase up to 20 wt% (1.46). Up to 25 wt%, a further slight decrease is observed (1.06). Although biodiesel already shows a reduction in soot compared to fossil diesel (decrease from 1.27 to reference fossil diesel fuel), a further significant reduction is achieved with solketal. In order to draw conclusions about combustion, the LOL and signal and ignition delays are taken into account. Both corresponding trends exhibit the same progression. The left side of Fig. 8 shows the LOL for both soot incandescense and OH* radicals. The LOL and ignition tend to increase with higher solketal content for OH* radical chemiluminescence. The LOL increases in the range from 1.2 to 1.4, while the ignition delay increases to 1.25 for 25 wt% solketal. An exception is the ignition delay at 10 wt% solketal, which shows a slight decrease of 1.03. This behavior contrasts with the behavior of soot incandescense and its signal delay, where the same trend occurs, but in the opposite direction. As the ignition delay increases, the signal delay decreases. The signal delay changes are in the range of 1.01 to 1.03. The progression of the LOL for the soot incandescense displays variation factors in the range of 1.06 to 1.14. Due to the increase in ignition delay caused by higher solketal content, higher LOL values are achieved, resulting in better mixing of the fuel-oxygen ratio. This can lead the premixed combustion to take place more effectively because of the higher fuel oxygen [58]. As a result, there should be increased formation of OH* radicals. However, as OH* radical values decrease, solketal can be expected to have a soot-reducing effect. The comparison with reference fossil diesel fuel and 1,3-dioxolane already implied that solketal has a soot-reducing effect due to its oxygen content and hydroxyl group. This observation was confirmed by increasing the solketal content in a biodiesel matrix. Furthermore, this study shows in detail that solketal also promotes better mixing of fuel and oxygen due to the extension of the ignition delay and should therefore operate leaner.

3.4. Influence of solketal on the ignition behavior of diesel R33

In order to confirm the soot-reducing tendency observed in the previous sections, the system is now being expanded to include HVO and fossil diesel. For this purpose, solketal is used in a commercially available fuel containing these components, namely Diesel R33. As in the previous study, the injection settings of 62 bar ambient pressure, 627 °C ambient temperature and an injection pressure of 1,500 bar at a fuel temperature of 90 °C were selected. The influence of solketal was taken into account in the range between 2 and 9 wt%. Figs. 9 to 10 show the soot incandescense, OH* radical chemiluminescence, LOL as well as the ignition and signal delays. When looking at soot incandescense and OH* chemiluminescence, it can generally be seen that the addition of solketal leads to a reduction. This observation correlates with the previous

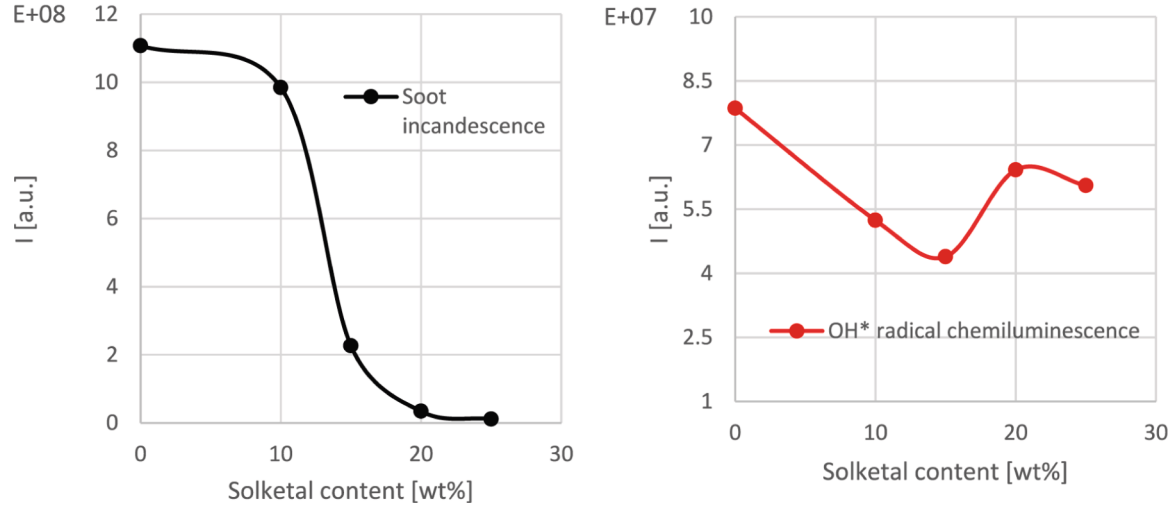

Fig. 7. The evolution of soot incandescense (left) and OH* radical chemiluminescence (right) for the binary biodiesel-solketal system for increasing solketal content. The injection conditions conducted ambient conditions of 62 bar and 627 °C, an injection pressure of 1,500 bar and a fuel temperature of 90 °C. The energizing time was 1500 µs.

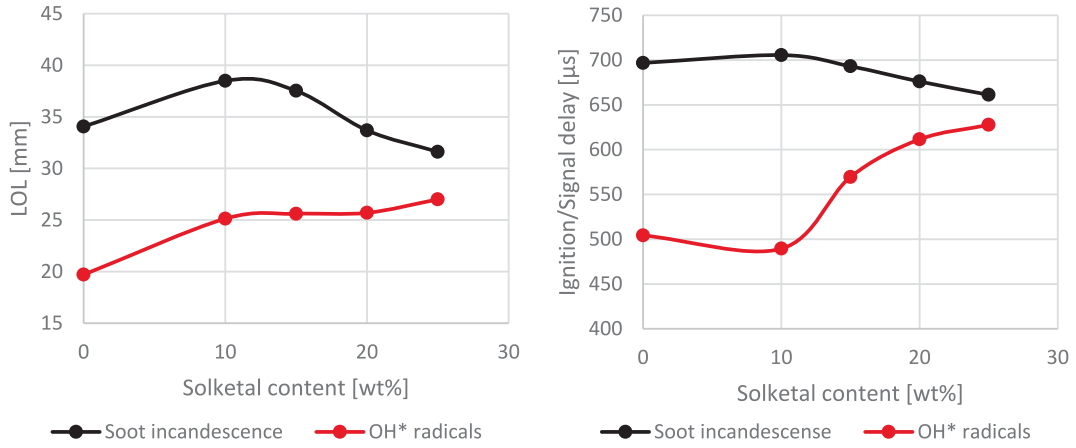

Fig. 8. Left: The LOL for the binary biodiesel-solketal system with increasing solketal content. The values for soot incandescense are shown in black and those for OH* radical chemiluminescence in red. Right: Progress of signal delay (soot incandescense, black) and ignition delay (OH* radical, red) for the binary biodiesel-solketal system increasing solketal content. The injection conditions conducted ambient conditions of 62 bar and 627 °C, an injection pressure of 1,500 bar and a fuel temperature of 90 °C. The energizing time was 1500 µs. (For interpretation of the references to colour in this figure legend, the reader is referred to the web version of this article.)

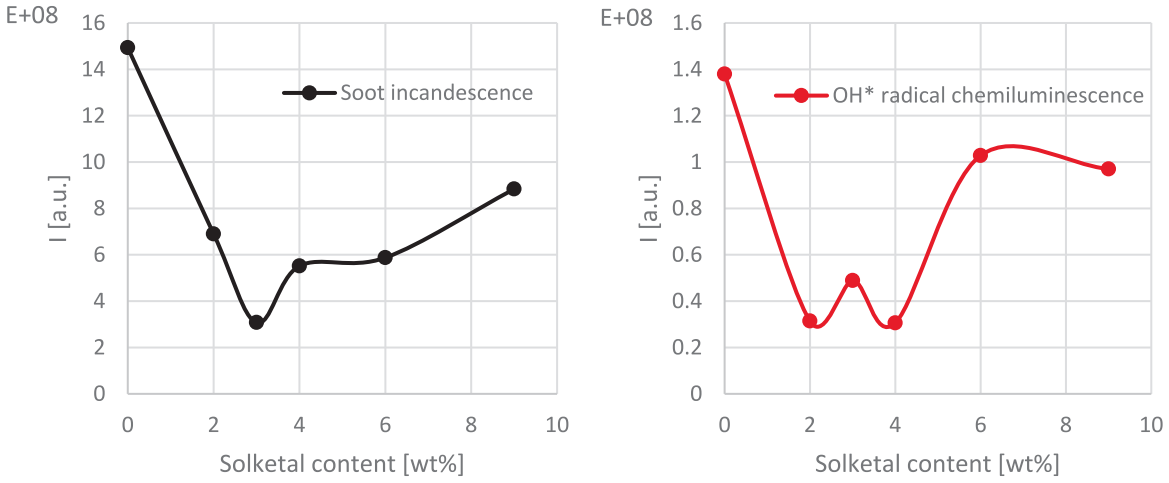

Fig. 9. The evolution of soot incandescense (left black,) and OH* radical chemiluminescence (right, red) for the Diesel R33 system for increasing solketal content. The injection conditions conducted ambient conditions of 62 bar and 627 °C, an injection pressure of 1,500 bar and a fuel temperature of 90 °C. The energizing time was 1500 µs. (For interpretation of the references to colour in this figure legend, the reader is referred to the web version of this article.)

sections and should occur due to the increase in molecular oxygen density. Interestingly, both, soot incandescense and OH* radical chemiluminescence show a deviant behavior at 3 wt% S. For soot incandescense, a minimum is reached here for the entire measurement, while for the OH* radical it represents a local maximum between 2 and 4 wt% S. Compared to Diesel R33, the signal for soot incandescense is reduced by a factor of 4. In comparison with R33 + 2 wt% S, the values decreased by 1.9 and compared to Diesel R33 + 4 wt%, they increased by 1.8. Subsequently, the trend rises again with higher solketal content, except for Diesel R33 + 6 wt% S, which decreases minimally by a factor of 1.2. In the case of the OH* radical, the addition of 2 wt% S leads to a significant decrease by a factor of 4.39. The maximum is then reached at 3 wt% S, which corresponds to an increase of 1.56 and subsequently decrease of 1.60. Afterwards, the formation increases significantly by 3.36 at 6 % by weight, followed by a slight decrease of 1.06 at 9 wt% S. The ignition and signal delay correlates with both parameters. A minimum was also observed for diesel R33 + 3 wt% S. Compared to pure Diesel R33, this blend is the only one that ignites faster (1.09). All other solketal contents ignite later than Diesel R33. The consideration of the LOL emphasizes the special blending behavior. Here, the LOL for OH* radical chemiluminescence shows that there is a continuous increase in the range from 1.01 to 1.06. The LOL for soot incandescense behaves somewhat differently, initially decreasing before reaching a maximum at 3 wt% S. It then decreases again before rising again at 6 and 9 wt% S, similar to OH* radical chemiluminescence. The correlation between ignition delay and OH LOL indicates a special interaction. Although the fuel ignites most rapidly here, there is better mixing between fuel and air. This correlation then leads to a minimum in soot incandescense. Interestingly, at higher solketal contents, the tendency to form soot increases again despite the rising solketal content. The fact that the quaternary system behaves differently indicates an additional interaction between the hydrocarbons and biodiesel and solketal. However, it is difficult to draw mechanistic conclusions, as increases of 1 wt% represent a change in soot formation tendency. Therefore, this does not indicate a cause related to the mixing ratios. It is more likely that this is a kinetic phenomenon. In general, there are anomalies in the interaction between fuel components, as can be seen, for example, in the B20 effect [59,60]. A biodiesel concentration of 20 % leads to a maximum in precipitation, which in turn results in an increase in mutagenic emission. The same applies to biodiesel concentrations, which showed, for example, that NOx emissions can be minimal at a biodiesel content of 15 % [61]. This shows that the addition of 3 wt% solketal to Diesel R33 has the potential

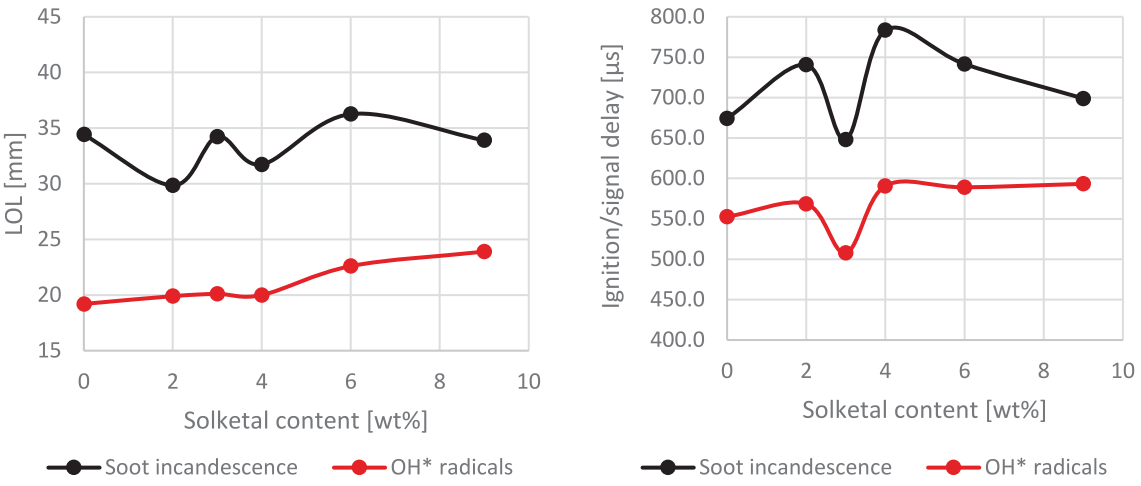

Fig. 10. Left: The LOL for the Diesel R33 system with increasing solketal content. Right: Progress of signal delay (soot incandescense) and ignition delay (OH* radical) for the Diesel R33 system increasing solketal content. The values for soot incandescense are shown in black and those for OH* radical chemiluminescence in red. The injection conditions conducted ambient conditions of 62 bar and 627 °C, an injection pressure of 1,500 bar and a fuel temperature of 90 °C. The energizing time was 1500 µs. (For interpretation of the references to colour in this figure legend, the reader is referred to the web version of this article.)

to produce low-soot fuel.

4. Conclusion and outlook

Investigations on solketal's influence on soot incandescense and OH* radical chemiluminescence, both in terms of its delay and LOL, showed that solketal exhibits soot-reducing tendencies. The variation in injection parameters showed essentially the same trend for the reference fossil diesel fuel and the 3 wt% blends with 1,3-dioxolane and solketal. In addition, 1,3-dioxolanes and solketal exhibit similar behavior, However, the low-energy states imply that solketal is more reactive in terms of its oxidative properties. Furthermore, a comparison between 1,3-dioxolane and solketal suggests that the additional hydroxyl group decreases soot formation. Looking at the lift off lengths emphasizes this observation, as they show that the two blends have the same length, making an air–fuel mixture effect less likely. Solketal shows mostly an increase in ignition delay compared to the reference fossil diesel fuel and a decrease for 1,3-dioxolane. The impact of solketal at higher concentrations revealed that increasing the solketal content reduces the soot content in binary biodiesel-solketal blends. This becomes apparent when all parameters are considered in correlation. In addition, the blends ignited at a concentration of up to 25 wt%. The investigation in a quaternary blend with HVO and fossil diesel fuel also showed soot-reducing properties. Furthermore, it was found that the best ignition and soot formation properties occur at a solketal content of 3 wt%.

After determining the ignition characteristics of blends with solketal in an injection chamber, the next step is to conduct engine test benches. The focus should be on further investigations to examine the influence of hydroxyl groups. Fundamental investigations such as shock tube tests, rapid compression machine tests and kinetic investigations must be carried out. In addition, due to the trade-off with soot, other emissions such as NO_x should be investigated. Furthermore, the behavior of the optimum for Diesel R33 + 3 wt% S remains to be investigated in greater detail. The focus should be on the influence of each of the four fuel components on ignition characteristics and combustion. Furthermore, the interactions between the components should be evaluated, as these hold the potential to design an ideal fuel.

CRediT authorship contribution statement

Julian Türck: Writing – original draft, Methodology, Investigation, Data curation, Conceptualization. **Sebastian Riess:** Writing – review & editing, Visualization, Investigation, Formal analysis, Data curation. **Lukas Strauß:** Writing – review & editing, Formal analysis, Data curation. **Fabian Schmitt:** Writing – review & editing, Validation, Methodology. **Ralf Türck:** Writing – review & editing, Project administration, Funding acquisition. **Wolfgang Ruck:** Supervision, Project administration. **Michael Wensing:** Writing – review & editing, Supervision, Project administration. **Jürgen Krahl:** Writing – review & editing, Supervision, Project administration, Methodology, Funding acquisition, Conceptualization.

Declaration of competing interest

The authors declare that they have no known competing financial interests or personal relationships that could have appeared to influence the work reported in this paper.

Appendix A. Supplementary data

Supplementary data to this article can be found online at https://doi.org/10.1016/j.ecmx.2026.101714.

Data availability

Data will be made available on request.

References

[1] Karatzos S, et al. Drop-in biofuel production via conventional (lipid/fatty acid) and advanced (biomass) routes. Part I. Biofuels Bioprod Biorefin 2017;11(2):344–62.
[2] Kass MD, et al. Compatibility assessment of fuel system elastomers with bio-oil and diesel fuel. Energy Fuel 2016;30(8):6486–94.
[3] Birgel A, et al. Investigations on deposit formation in the holes of diesel injector nozzles. SAE Int J Fuels Lubr 2012;5(1):123–31.
[4] Götz K, et al. (2016). Exhaust Gas Emissions and Engine Oil Interactions from a New Biobased Fuel Named Diesel R33, SAE Technical Paper.
[5] Weyhing T, et al. (2021). reFuels–rethinking fuels: Performance of regenerative fuels. Internationaler motorenkongress 2021, Springer: 569-577.
[6] Omari A, et al. Potential of long-chain oxymethylene ether and oxymethylene ether-diesel blends for ultra-low emission engines. Appl Energy 2019;239:1242–9.
[7] Liu S, et al. Study of spark ignition engine fueled with methanol/gasoline fuel blends. Appl Therm Eng 2007;27(11–12):1904–10.
[8] Lemaire R, et al. Effect of ethanol addition in gasoline and gasoline–surrogate on soot formation in turbulent spray flames. Fuel 2010;89(12):3952–9.
[9] De Poures MV, et al. Using renewable n-octanol in a non-road diesel engine with some modifications. Energy Sources Part A 2019;41(10):1194–208.
[10] Steinmetz SA, et al. Crude glycerol combustion: particulate, acrolein, and other volatile organic emissions. Proc Combust Inst 2013;34(2):2749–57.
[11] Coronado CR, et al. Ecological efficiency in glycerol combustion. Appl Therm Eng 2014;63(1):97–104.

[12] Jaecker-Voirol A, et al. Glycerin for new biodiesel formulation. Oil Gas Sci Technol-Revue De l'IFP 2008;63(4):395–404.
[13] Alptekin E. Emission, injection and combustion characteristics of biodiesel and oxygenated fuel blends in a common rail diesel engine. Energy 2017;119:44–52.
[14] Nanda MR, et al. Catalytic conversion of glycerol for sustainable production of solketal as a fuel additive: a review. Renew Sustain Energy Rev 2016;56:1022–31.
[15] Song J, et al. Comparison of the impact of intake oxygen enrichment and fuel oxygenation on diesel combustion and emissions. Energy Fuel 2004;18(5):1282–90.
[16] Alptekin E, Canakci M. Performance and emission characteristics of solketal-gasoline fuel blend in a vehicle with spark ignition engine. Appl Therm Eng 2017;124:504–9.
[17] Vichare MS, et al. Solketal-diesel nanoemulsion as fuel for diesel engine: a study on the emulsion stability, engine performance, and emission characteristics. J Dispers Sci Technol 2025:1–10.
[18] Mota CJ, et al. Glycerin derivatives as fuel additives: the addition of glycerol/acetone ketal (solketal) in gasolines. Energy Fuel 2010;24(4):2733–6.
[19] Türck J, et al. Solketal as a renewable fuel component in ternary blends with biodiesel and diesel fuel or HVO and the impact on physical and chemical properties. Fuel 2022;310:122463.
[20] Türck J, et al. Extension of biodiesel aging mechanism–the role and influence of Methyl Oleate and the contribution of Alcohols through the use of Solketal. ChemSusChem 2023;16(17):e202300263.
[21] Kerkel F, et al. Stabilisation of biofuels with hydrophilic, natural antioxidants solubilised by glycerol derivatives. Fuel 2021;284:119055.
[22] Türck J, et al. Investigation of the spray formation of solketal under diesel engine conditions and the influence on Diesel R33. Fuel Process Technol 2025;277:108308.
[23] Santhoshkumar A, et al. (2019). Performance, combustion, and emission characteristics of DI diesel engine using mahua biodiesel. Advanced Biofuels, Elsevier: 291-327.
[24] Cataluna R, Da Silva R. Effect of cetane number on specific fuel consumption and particulate matter and unburned hydrocarbon emissions from diesel engines. J Combust 2012;2012(1):738940.
[25] O'Connor J, et al. Effect of post injections on mixture preparation and unburned hydrocarbon emissions in a heavy-duty diesel engine. Combust Flame 2016;170:111–23.
[26] Kashdan J, et al. An investigation of unburned hydrocarbon emissions in wall guided, low temperature diesel combustion. Oil Gas Sci Technol-Revue De l'IFP 2008;63(4):433–59.
[27] Imperato M, et al. Split fuel injection and Miller cycle in a large-bore engine. Appl Energy 2016;162:289–97.
[28] Al Ezzi A, et al. Influence of fuel injection pressure and RME on combustion, NOx emissions and soot nanoparticles characteristics in common-rail HSDI diesel engine. Int J Thermofluids 2022;15:100173.
[29] Azimov U, et al. Evaluation of the flame lift-off length in diesel spray combustion based on flame extinction. J Therm Sci Technol 2010;5(2):238–51.
[30] Liu H, Zheng S. Measurement of temperature and wavelength-dependent emissivity distributions using multi-wavelength radiation thermometry. Opt Commun 2020;472:125895.
[31] Dec JE. Advanced compression-ignition engines—understanding the in-cylinder processes. Proc Combust Inst 2009;32(2):2727–42.
[32] Bockhorn H. Soot formation in combustion: mechanisms and models. Springer Science & Business Media; 2013.
[33] Xia Y, et al. Emission characteristics of confined non-premixed ammonia–oxygen–nitrogen turbulent jet flames under oxygen-enriched conditions. Proc Combust Inst 2024;40(1–4):105704.
[34] Yuan H, et al. Study on soot nucleation and growth from PAHs and some reactive species at flame temperatures by ReaxFF molecular dynamics. Chem Eng Sci 2019;195:748–57.
[35] Hardalupas Y, Orain M. Local measurements of the time-dependent heat release rate and equivalence ratio using chemiluminescent emission from a flame. Combust Flame 2004;139(3):188–207.
[36] Riess S, et al. Air entrainment and mixture distribution in diesel sprays investigated by optical measurement techniques. Int J Engine Res 2018;19(1):120–33.
[37] Tonti F, et al. Obtaining pseudo-OH* radiation images from CFD solutions of transcritical flames. Combust Flame 2021;233:111614.
[38] Sharipov AS, et al. A detailed kinetic submechanism for OH* chemiluminescence in hydrogen combustion revisited. Part 1. Combust Flame 2024;263:113407.
[39] Bowden J, et al. (1974). Octane-cetane relationship.
[40] Rieß S. Einfluss von Kraftstoff und Abgasrückführung auf Gemischbildung und Verbrennung von dieselmotorischen Sprays. Shaker Verlag; 2017.
[41] Yang K, et al. Effects of ambient conditions on the ignition and combustion characteristics of ignited natural gas under methane atmosphere. Energy 2024;313:133976.
[42] Alias MHR, et al. (2018). Effect of injection pressure, injection duration, and injection frequency on direct injector's mass flow rate for compressed natural gas fuel. MATEC web of conferences, EDP Sciences.
[43] Wang L, et al. High injection pressure diesel sprays from a piezoelectric fuel injector. Appl Therm Eng 2019;152:807–24.
[44] Liu L, et al. Kinetic mechanism and experimental study of initial temperature and blended gas addition on combustion characteristics of coal bed methane-air. Combust Sci Technol 2025:1–18.
[45] Tuan NV, et al. Evaluate the influence of several parameters on the HCCI combustion process in a constant volume combustion chamber. Discover Appl Sci 2025;7(4):258.
[46] Fan C, et al. Chemical feature of the soot emissions from a diesel engine fueled with methanol-diesel blends. Fuel 2021;297:120739.
[47] Kumar P, et al. Study of performance parameters and emissions of four stroke CI engine using solketal-biodiesel blends. SN Appl Sci 2021;3(1):59.
[48] Glassman I. (1989). Soot formation in combustion processes. Symposium (international) on combustion, Elsevier.
[49] Bobba MK, et al. Effect of ignition delay on in-cylinder soot characteristics of a heavy duty diesel engine operating at low temperature conditions. SAE Int J Engines 2009;2(1):911–24.
[50] Cie L. "1,3-Dioxolane." from https://www.lambiotte.com/dioxolane/.
[51] Glaconchemie. "Glycasol." from https://glaconchemie.de/produkte/glycerin-derivate/glyca-sol#:~:text=GLACONCHEMIE%20wird%20GLYCASOL%C2%AE%20%2F%20Isopropylidenglycerin,somit%2068%2C2%20%25%20betragen.
[52] Scientific F. "Solketal." from https://www.fishersci.com/shop/products/solketal-97-thermo-scientific-1/AC153651000.
[53] Berteau C, et al. Evaluation of the impact of viscosity, injection volume, and injection flow rate on subcutaneous injection tolerance. Med Devices: Evidence Res 2015:473–84.
[54] Pandey RK, et al. Impact of alternative fuel properties on fuel spray behavior and atomization. Renew Sustain Energy Rev 2012;16(3):1762–78.
[55] Sukjit E, et al. Finding synergies in fuels properties for the design of renewable fuels–hydroxylated biodiesel effects on butanol-diesel blends. Environ Sci Technol 2013;47(7):3535–42.
[56] Martos F, et al. Impact of alcohol–diesel fuel blends on soot primary particle size in a compression ignition engine. Fuel 2023;333:126346.
[57] Trifoi AR, et al. Glycerol acetals and ketals as possible diesel additives. a review of their synthesis protocols. Renew Sustain Energy Rev 2016;62:804–14.
[58] Zhu H, et al. Effect of fuel oxygen on the trade-offs between soot, NOx and combustion efficiency in premixed low-temperature diesel engine combustion. Fuel 2013;112:459–65.
[59] Krahl J, et al. (2008). Exhaust gas emissions and mutagenic effects of diesel fuel, biodiesel and biodiesel blends, SAE Technical Paper.
[60] Schmidt L. (2014). Wechselwirkungen zwischen Kraftstoffkomponenten in biodieselbasierten Mischkraftstoffen unter besonderer Berücksichtigung der Alterungsprodukte von Fettsäuremethylestern, Cuvillier Verlag.
[61] Lahane S, Subramanian K. Effect of different percentages of biodiesel–diesel blends on injection, spray, combustion, performance, and emission characteristics of a diesel engine. Fuel 2015;139:537–45.